Journal of Coastal Research	35	2	314–321	Coconut Creek, Florida	March 2019

Impacts of Tidal Flat Reclamation on Saltwater Intrusion and Freshwater Resources in the Changjiang Estuary

Hanghang Lyu and Jianrong Zhu*

State Key Laboratory of Estuarine and Coastal Research
East China Normal University
Shanghai 200062, PR China

Shanghai Institute of Eco-Chongming
Shanghai 200062, PR China

www.cerf-jcr.org

www.JCRonline.org

ABSTRACT

Lyu, H. and Zhu, J., 2019. Impacts of tidal flat reclamation on saltwater intrusion and freshwater resources in the Changjiang Estuary. *Journal of Coastal Research,* 35(2), 314–321. Coconut Creek (Florida), ISSN 0749-0208.

A well-validated numerical model, residual water and salt transport, and the water diversion ratio between channels as well as their variations were used to simulate and analyze the impacts of the tidal flat reclamation project in the Eastern Hengsha Shoal (RP-EHS) on saltwater intrusion and freshwater resources. The RP-EHS is the largest tidal flat reclamation project in the Changjiang Estuary and has significantly changed the local topography. The RP-EHS results in a net transection water flux increase in the North Channel and decreases in the South Channel, North Passage, and South Passage, which weaken the saltwater intrusion in the North Channel and enhance the saltwater intrusion in the South Channel, North Passage, and South Passage. The saltwater intrusion in the North Branch and the saltwater spillover from the North Branch into the South Branch were increased after the establishment of the RP-EHS. There are three reservoirs in the Changjiang Estuary, which provide more than 80% of the freshwater to Shanghai. Because the saltwater sources of the reservoirs mainly originate from the saltwater spillover, the salinity at the water intakes of the three reservoirs slightly increased after the project, which means that the project is unfavorable for water resources in the Changjiang Estuary. The reservoirs are important for Shanghai's water supply, and the impacts of the tidal flat reclamation on water resources should receive greater attention to ensure water safety.

ADDITIONAL INDEX WORDS: *Reclamation project, numerical model, residual transport, salinity, water safety.*

INTRODUCTION

The Changjiang, which is also known as the Yangtze River, is one of the largest rivers in the world. The Changjiang Estuary has a 90-km-wide river mouth and is characterized by multiple bifurcations with large tidal flats (Figure 1). The estuary is bifurcated by Chongming Island into the South Branch and North Branch. The South Branch and its lower reaches form the main channel of the Changjiang and contribute to most of the river discharge, while the North Branch is heavily silted, has a funnel shape in the lower reaches and is almost orthogonal to the South Branch in the upper reaches. Then, the lower South Branch is bifurcated into the South Channel and the North Channel by Changxing Island and Hengsha Island. Finally, the South Channel is bifurcated into the South Passage and North Passage by Jiuduansha Island. Widespread tidal flats occur near the river mouth, which include the Eastern Chongming Shoal, Eastern Hengsha Shoal, and Nanhui Shoal.

Shanghai is an international megalopolis located near the Changjiang Estuary and has endured land resource shortages. To reduce this problem, tidal reclamation projects in the Changjiang Estuary were conducted. The largest reclamation project is the Eastern Hengsha Shoal (RP-EHS) (Figure 1). The RP-EHS began in December 2003, and now, 182 km^2 of tidal flats are enclosed.

Many tidal flat reclamation projects occur in other estuaries and bays of the world, and they have shown that they had significant influences on hydrodynamic processes. For example, these were the reclamations in the innermost part of the Ariake Sound, Japan, which caused the tidal currents to decrease by more than 10% over a large area in the innermost part of the sound (Manda and Matsuoka, 2006). The reclamation of portions of the Tokyo Bay, Japan, decreased the residence time of seawater by 35% (Okada *et al*., 2011). Zainal *et al*. (2012) assessed the ecological and economic impacts of land reclamation and dredging in the Kingdom of Bahrain and found that the estimated total cumulative loss of major habitats (seagrass, algal beds, rocks, and corals) resulting from the 10 selected reclamation and dredging projects was around 153.58 km^2. The reclamation on the west coast of Korea generated the far-field effects on the Chinese coast and could result in a rise of tidal amplitude and onshore sediment transport. The former may enhance the coastal hazards such as storm surge, and the latter may result in severe siltation (Song *et al*., 2013). van Maren *et al*. (2016) studied the effect of land reclamations and sediment extraction on the suspended sediment concentration in the Ems Estuary on the Dutch-German border and revealed that a decrease in accommodation space for fine-grained sediments by land reclamations or by reducing fine-grained sediment extraction would lead to an increase in suspended sediment concentrations. The reclamation and other anthropogenic projects in the San Francisco Estuary had effects on saltwater intrusion and outflow because of the changes in estuary geometry, bathymetry, and tidal trapping (Andrews, Gross, and Hutton, 2017). Saltwater intrusion can produce

DOI: 10.2112/JCOASTRES-D-18-00077.1 received 8 June 2018; accepted in revision 15 September 2018; corrected proofs received 18 October 2018; published pre-print online 30 November 2018.
*Corresponding author: jrzhu@sklec.ecnu.edu.cn

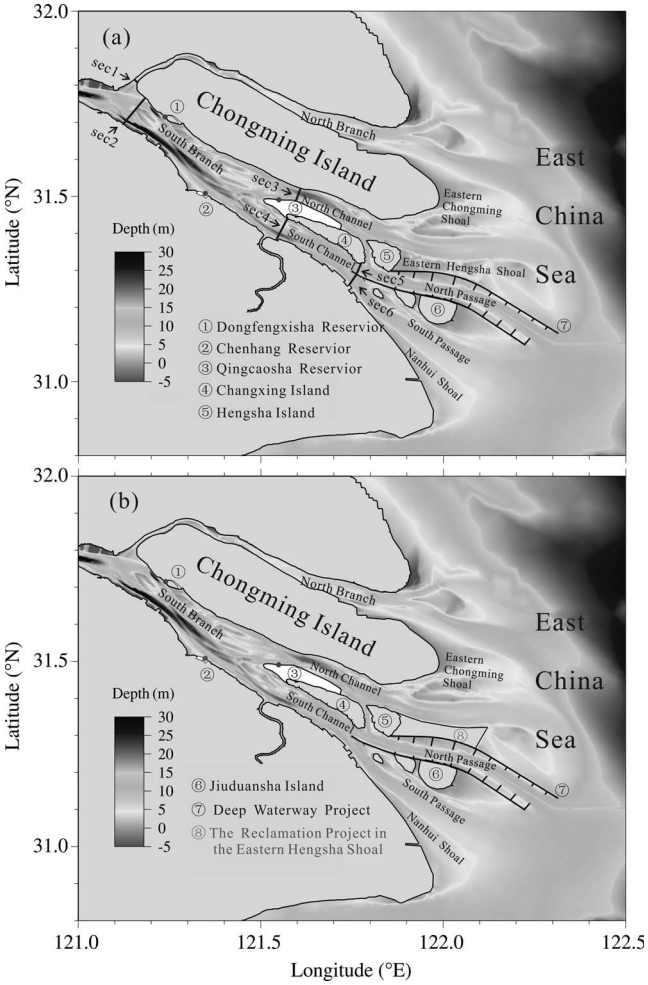

Figure 1. Topography of the Changjiang Estuary before (a) and after (b) the RP-EHS. Black dots indicate the locations of water intakes of the reservoirs; the cross-channel sects for later analyses are marked by the black lines.

estuarine circulation (Pritchard, 1956) and effect stratification (Simpson *et al*., 1990); thereby, saltwater intrusion influences sediment transport and produces peak estuarine turbidities (Geyer, 1993).

Saltwater intrusion in the Changjiang Estuary is mainly controlled by river discharge and tides (Li *et al*., 2010; Qiu, Zhu, and Gu, 2012; Shen, Mao, and Zhu, 2003; Wu *et al*., 2006; Zhu *et al*., 2010) but is also influenced by wind (Li *et al*., 2012), topography (Li *et al*., 2014), river basin and estuarine projects (Qiu and Zhu, 2013; Zhu *et al*., 2006), and sea-level rise (Qiu and Zhu, 2015). There is a particular type of saltwater intrusion, which is the saltwater spillover from the North Branch into the South Branch that occurs during spring tide in dry season (Shen, Mao, and Zhu, 2003; Wu *et al*., 2006; Wu and Zhu, 2007; Wu, Zhu, and Choi, 2010). Only a small amount of the saltwater returns to the North Branch because the shoals in the upper reaches of the North Branch are exposed to the air during ebb tide. The saltwater that spilled into the South Branch is transported downstream by runoff and arrives in the middle reaches of the South Branch during the subsequent neap tide. Together with the saltwater spillover, the landward saltwater intrudes in the North Channel, North Passage, and South Passage, which threatens the security of freshwater resources, *i.e*. the Qingcaosha Reservoir, Chenhang Reservoir, and Dongfengxisha Reservoir. The Qingcaosha Reservoir is a massive reservoir, which is located in the upper North Channel and along the NW portion of Changxing Island. The reservoir was completed in 2010 and provides domestic water usage for 13 million people in Shanghai; however, this reservoir is frequently threatened by saltwater intrusion during dry season. Water from the Changjiang can flow into the reservoirs when the salinity is lower than 0.45 psu, which is the salinity standard for drinking water, but this operation is suspended when saltwater intrusion influences the water intake. These reservoirs use the difference of water level between inside and outside of the reservoir by water gates. The gates are open when there is freshwater outside the gates and water level outside the gates is higher than the one inside the gates. Otherwise, the gates are closed. The dam of these reservoirs cannot be overtopped by the outside river water.

Although many studies of saltwater intrusion in the Changjiang Estuary have been conducted, the influence of the RP-EHS on saltwater intrusion and water resources remains unclear. The RP-EHS is a huge tidal flat reclamation project. Many tidal flat reclamation projects in other estuaries and bays of the world have been conducted and will have been performed. This study can promote people's understanding on the affects of tidal flat reclamations on the estuary and provide a reference to explain some similar phenomenon in other regions.

In this study, the influence of the RP-EHS on residual water transport, salt transport, and saltwater intrusion in the Changjiang Estuary are assessed by a three-dimensional (3D) hydrodynamic numerical model. The remainder of this paper is organized as follows. In the "Methods" section, the numerical model and experiments are described. In the "Results" section, the effect of the RP-EHS on residual water transport, salt transport, and the water diversion ratio (WDR) between channels and saltwater intrusion are analyzed and discussed. In the "Discussion" section, the impacts of the RP-EHS on water resources are discussed. Finally, the conclusions are presented.

METHODS

The 3D, semi-implicit estuarine, coastal, and ocean model (ECOM-si; Blumberg, 1994) which originated from the Princeton Ocean Model (Blumberg and Mellor, 1987) was applied in this study. The high-order spatial interpolation at the middle temporal (HSIMT) level coupled with a total variation diminished (TVD) limiter (HSIMT-TVD) of advection scheme used the ECOM-si model, which is useful for solving the transport equations and also significantly reducing the numerical diffusions with third-order accuracy (Wu and Zhu, 2010). The model used sigma coordinates in vertical direction and a curvilinear non-orthogonal grid in the horizontal direction (Chen *et al*., 2004). The modified Mellor and Yamada level 2.5 turbulence closure scheme (Galperin *et al*., 1988; Mellor and Yamada, 1982) was implemented in the model to calculate the vertical eddy viscosity and diffusivity coefficients.

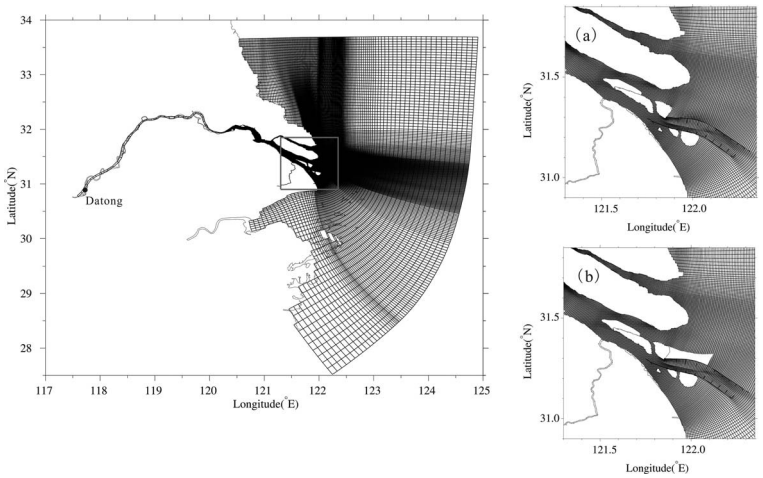

Figure 2. Numerical model grid. Enlarged views of the model grid around the tidal reclamation project (a) before the RP-EHS and (b) after the RP-EHS.

A wet/dry scheme was included to describe the intertidal area with a critical depth of 0.1 m (Zheng, Chen, and Liu, 2003; Zheng, Chen, and Zhang, 2004).

The model domain covered the entire Changjiang Estuary, Hangzhou Bay, and the seas adjacent to these areas (see Figure 2). The model domain extended east to 124.9°E, north to 33.7°N, south to 27.5°N, and west to the Datong gauge station. In this study, the total cell number was refined to 337×225 in the horizontal direction with 10 uniform sigma layers in the vertical direction to better resolve the topography around the river mouth. The model grids are nearly orthogonal and smooth all over, and the grids fit the shape of the coastline in the bifurcated channels and near the deep waterway project. Resolutions varied from 300 to 500 m around the river mouth, and then, the resolution gradually decreased to 10 km at the open sea boundary. The integrated time step was set to 20 seconds.

The tide comprising the 16 astronomical tidal constituents (M_2, S_2, N_2, K_2, K_1, O_1, P_1, Q_1, MU_2, NU_2, T_2, L_2, $2N_2$, J_1, M_1, and OO_1) were obtained through harmonic analysis to drive the open sea boundary. In the 16 total tidal constituents, the eight main tidal constituents are M_2, S_2, N_2, K_2, K_1, O_1, P_1, and Q_1, respectively. This group has done some work on this research before (Zhang, Zhu, and Wu, 2005). The M_2, S_2, N_2, and K_2 accounts for more than 80% of the tide constituted by the 16 tidal constituents in the East China Sea. Daily river discharge recorded at the Datong Station was used in the model as the river boundary condition. Wind data with a resolution of 0.5°×0.5° were adopted based on a semimonthly mean of 10 years from the National Centers for Environmental Prediction data (Saha *et al*., 2010). The initial salinity distribution was derived from the Ocean Atlas in Huanghai Sea and East China Sea (Hydrology) (Editorial Board for Marine Atlas, 1992) outside the Changjiang mouth and from the observed data of the inner river mouth.

The authors' research group has conducted many model validations for the Changjiang Estuary, which have shown that the model can repeat the observed water level, current, and salinity quite well. The model validation in this study is omitted to save space, and thus, readers are referred to the literature for model validation (Li *et al*., 2014; Li, Zhu, and Wu, 2012; Lyu and Zhu, 2018; Qiu and Zhu, 2015).

Two numerical experiments were conducted: experiments before the RP-EHS and after the RP-EHS. The model calculation start date is 10 December 2014, and the end date is 28 February 2015. The modeled data for February was output to analyze and compare the impacts of the RP-EHS on the residual water transport, salt transport, WDR, and saltwater intrusion. The river discharges in December, January, and February were assigned using the monthly mean values since 1950, which were measured at the Datong hydrological gauging station; these values are 13,600, 11,100, and 12,000 m^3/s, respectively.

To better describe the water subtidal movements, the instantaneous rate of water transport per unit width through a water column is defined as follows:

$$\vec{Q} = \int_{-1}^{0} H\vec{V}d\sigma \tag{1}$$

where, H is the total water depth, $\vec{V}$ is the current vector, and σ is the relative depth (0 at the surface and –1 at the bottom). Then, the residual unit width water flux (RUWF) is calculated as follows:

$$RUWF = \frac{1}{T}\int_{0}^{T} \vec{Q}dt \tag{2}$$

Similarly, the residual unit width salt flux (RUSF) is calculated as follows:

$$RUSF = \frac{1}{T}\int_{0}^{T} \vec{Q}s\,dt \tag{3}$$

where, T is the time period (which equals one or several tidal cycles), and s is salinity. In this study, six semidiurnal tidal

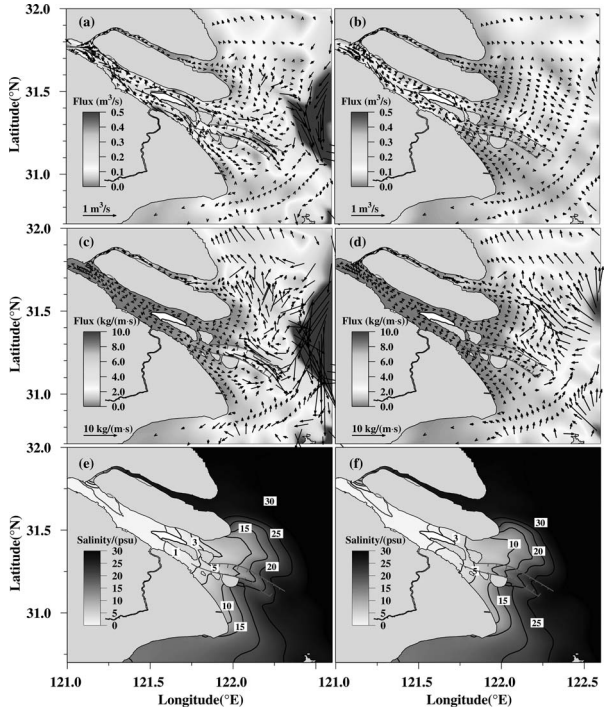

Figure 3. Distribution of RUWF (a, b), RUSF (c, d), and salinity (e, f) in the surface (left panel) and bottom (right panel) layer during spring tide before the RP-EHS. The isohalines are 0.45, which is the standard salinity of drinking water.

cycles (the reference point is the water intake of the Qingcaosha Reservoir, as shown in Figure 1) were used as an averaging time window to remove the semidiurnal and diurnal tidal signals.

To calculate the WDR between channels, the residual (net) transection water flux (NTWF) (transection location labeled in Figure 1) needs to be determined. The NTWF is calculated as follows:

$$NTWF = \frac{1}{T}\int_0^T \int_{-H(x,y)}^{\zeta} \int_0^L \vec{V}_n(x,y,z,t)\, dl\, dz\, dt \qquad (4)$$

where, ζ is the surface elevation, L is the width of the transect, and $\vec{V}_n(x,y,z,t)$ is the velocity component normal to the transect.

RESULTS

To assess the influences of the RP-EHS on saltwater intrusion and freshwater in the Changjiang Estuary. The residual water transport, salt transport, and WDR were derived from numerical model.

RUWF, RUSF, Saltwater Intrusion, and WDR before the RP-EHS

During the spring tide, the surface RUWF flows seaward in the South Branch, North Channel, North Passage, and South Passage, but the RUWF flows landward in the North Branch because of its funnel shape and tidal Stokes transport (Qiu and Zhu, 2015), which means that the South Branch, North Channel, and South Channel are the main channels for river discharge into the sea (Figure 3a). The NTWF in the upper reaches of the North Branch is –664 m^3/s, and the WDR is –6.2% (Table 1), where the negative sign means that the water is transported into the South Branch from the North Branch. Between the North Channel and South Channel, most of the river water (72.9%) discharges into the sea through the North Channel (Table 2). Between the North Passage and South Passage, most of the river water (accounting for 71.0%) flows into the sea through the North Passage, and only 29.0% of the river water discharges into the sea through the South Passage. The RUWF to the east of Chongming Island flows northward because of tidal Stokes transport and tidal pumping transport (Qiu and Zhu, 2015). In the bottom layer, the RUWF in the South Branch is seaward but decreases because of bottom friction (Figure 3b). The RUWF at the river mouth is landward induced by a strong salinity front, which is the cause of the two-layer estuarine circulation (Pritchard, 1956). The RUWF flows seaward in the Eastern Hengsha Shoal and landward east of the Eastern Hengsha Shoal in the surface and bottom layers. The pattern of RUSF is similar to that of the RUWF (Figure 3c,d), and the RUSF magnitude out of the river mouth is much larger because of high salinity in that area. Along the northern side of the north dyke of the deep waterway project, a larger RUSF flows landward, bringing high salinity into the North Channel and Eastern Chongming Shoal. The North Branch is filled with highly saline water, and the saltwater spillover was simulated, which is caused by the RUWF and RUSF flowing into the South Branch from the North Branch in the upper reaches (Figure 3e,f). The diluted water northeastward extends east of Chongming Island, which corresponds to the RUSF. The saltwater intrusion is stronger in the bottom layer than in the surface layer near the river mouth. Among the South Passage, North Passage, and North Channel, the saltwater intrusion is the strongest in the South Passage and weakest in the North Channel.

Table 1. *NTWF and WDR in the North Branch and South Branch during spring and neap tide before and after the RP-EHS.*

	NTWF (m^3/s)				WDR (%)			
	Spring		Neap		Spring		Neap	
	NB	SB	NB	SB	NB	SB	NB	SB
Before	–664	11,341	208	12,873	–6.2	106.2	1.6	98.4
After	–679	11,355	207	12,874	–6.4	106.4	1.6	98.4
$\triangle_{\text{After-Before}}$	–15	14	–1	1	–0.2	0.2	0	0

Table 2. *NTWF and WDR in the North Channel and South Channel during spring and neap tide before and after the RP-EHS.*

	NTWF (m^3/s)				WDR (%)			
	Spring		Neap		Spring		Neap	
	NC	SC	NC	SC	NC	SC	NC	SC
Before	8064	3003	5831	6540	72.9	27.1	47.1	52.9
After	8952	2134	5927	6455	80.8	19.3	47.9	52.1
$\triangle_{\text{After-Before}}$	888	–869	96	–85	7.9	–7.9	0.8	-0.8

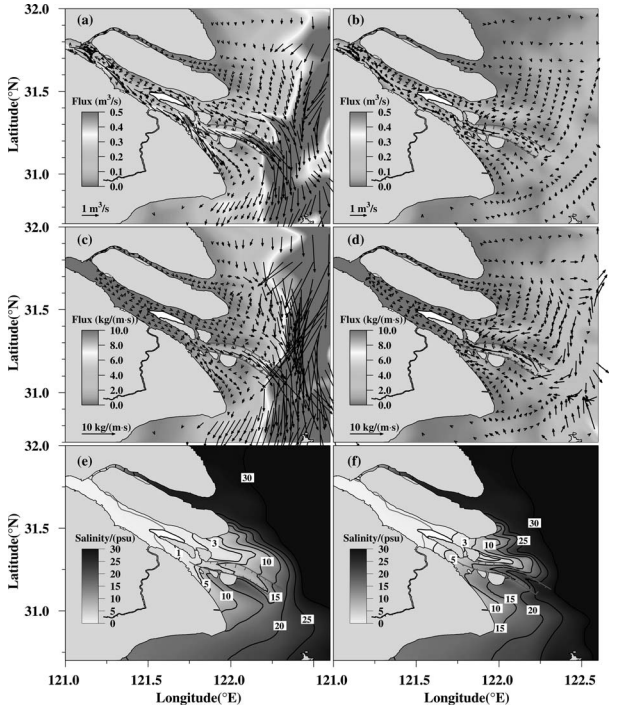

Figure 4. Distribution of RUWF (a, b), RUSF (c, d), and salinity (e, f) in the surface (left panel) and bottom (right panel) layer during neap tide before the RP-EHS. The isohalines are 0.45, which is the standard salinity of drinking water.

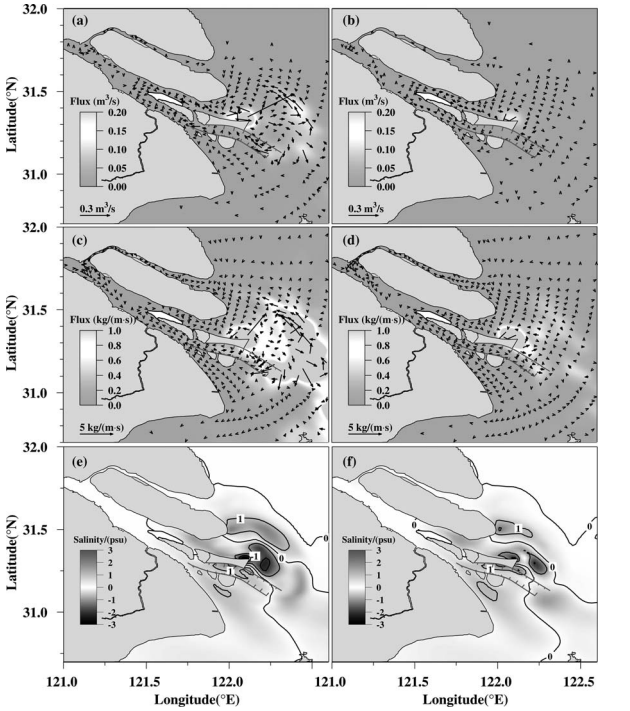

Figure 5. Difference distribution of RUWF (a, b), RUSF (c, d), and salinity (e, f) in the surface (left panel) and bottom (right panel) layer during spring tide between after and before the RP-EHS.

During neap tide (Figure 4), the RUWF and RUSF flow southward out of the river mouth in the surface layer and even in the bottom layer because the tide becomes weaker and the north wind effect is dominant (Wu *et al.*, 2014). The phenomenon seen in spring (Figure 5), namely, that RUWF and RUSF flow into the South Branch from the North Branch, disappears. The NTWF flows into the North Branch from the South Branch with 208 m^3/s of magnitude, and the WDR is 1.6% (Table 1). Between the North Channel and South Channel, more river water flows into the sea through the South Channel, which accounts for 52.9% (Table 2). Between the North Passage and South Passage, even more river water is transported downstream by the North Passage (Table 3), namely, 79.0%, because of the stronger salinity front in the South Passage that blocks the incoming river water flow. The landward RUWF and RUSF in the bottom layer become more distinct because of a much stronger horizontal salinity gradient. The saline water induced by the saltwater spillover, which occurs during the spring tide, is transported downstream by runoff and influences the water resources in the South Branch. The saltwater intrusion in the bottom layer near the river mouth is stronger than the one during the spring tide because of a weaker tide, which forms an observable saltwater wedge.

Table 3. *NTWF and WDR in the North Passage and South Passage during spring and neap tide before and after the RP-EHS.*

	NTWF (m^3/s)				WDR (%)			
	Spring		Neap		Spring		Neap	
	NP	SP	NP	SP	NP	SP	NP	SP
Before	2188	895	5079	1347	71	29	79	21
After	1562	654	5178	1166	70.5	29.5	81.6	18.4
$\triangle_{\text{After-Before}}$	–626	–241	99	–181	–0.5	0.5	2.6	–2.6

RUWF, RUSF, Saltwater Intrusion, and WDR after the RP-EHS

The distribution differences of the RUWF, RUSF, and salinity in the surface and bottom layers during spring tide are shown in Figure 6. The difference in RUWF and RUSF in the North Channel is seaward, which is the same direction as RUWF and RUSF before the RP-EHS and results in an overall salinity decrease in the North Channel. The reduced maximum salinity is greater than 1.0 psu NE of the project because the northern along-dyke water and salinity transport are weakened by the project. The NTWF and WDR in the North Channel are increased by 888 m^3/s and 7.9% (Table 2), which means more river water is bifurcated into the North Channel after the project and salinity decreases. The other reason for the salinity decrement in the North Channel is that the RP-EHS lengthens the North Channel, which leads the lower salinity water to flow further east of the area. The difference in the RUWF and RUSF over the Eastern Chongming Shoal is consistent with their directions before the project, which brings high salinity to that location and results in a salinity increase with the maximum value of more than 1.0 psu. In the South Channel, North Passage, and South Passage, the NTWFs are decreased by 869,

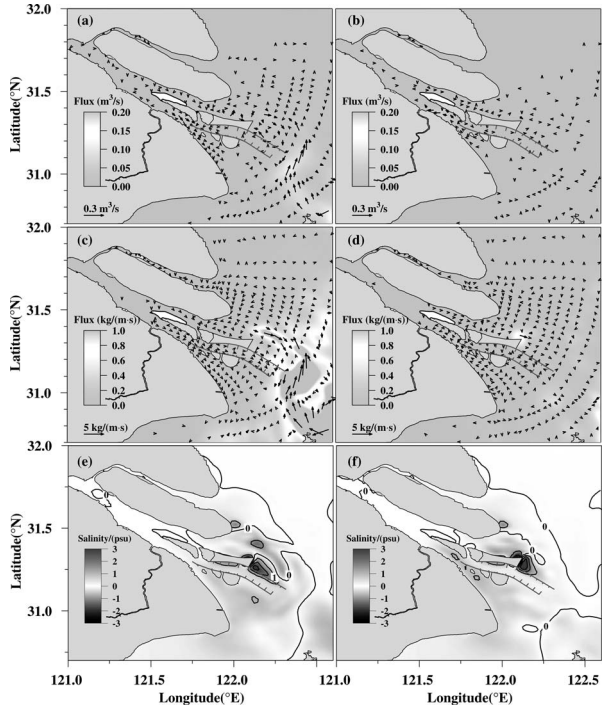

Figure 6. Difference distribution of RUWF (a, b), RUSF (c, d), and salinity (e, f) in the surface (left panel) and bottom (right panel) layer during neap tide between after and before the RP-EHS.

626, and 241 m^3/s (Table 2 and Table 3), respectively, resulting in a salinity increment of approximately 1.0 psu. In the North Passage south of the RP-EHS, the salinity increment reaches more than 1.0 psu because the lower salinity water in the North Channel is blocked from entering the North Passage over the north dyke by the RP-EHS. In the North Branch and South Branch, the differences in RUWF and RUSF are very small, and thus, the salinity change is small. At the upper reaches of the North Branch, the NTWF, which spills over from the North Branch into the South Branch, is increased by 15 m^3/s. The WDR also rises by 0.2% (Table 1), which indicates that the RP-EHS somewhat enhanced the saltwater intrusion in the North Branch and the saltwater spillover because of the salinity increment in its outer river mouth.

During neap tide, the patterns in the difference distribution of the RUWF, RUSF, and salinity in the surface and bottom layers are similar to those during spring tide, and the variation values decrease in most areas (Figure 7). The NTWF in the North Channel is increased only by 96 m^3/s, and the WDR is increased only by 0.8% (Table 2), which results in salinity increases in the North Channel and decreases in the South Channel, North Passage, and South Passage. The salinity east of the project is obviously increased because the lower salinity water blocks flow into that area because of the project. The NTWF is decreased by 181 m^3/s, and the WDR is reduced by 2.6% in the South Passage after the project (Table 3). At the upper reaches of the North Branch, the NTWF increases only by 1 m^3/s, and the WDR is hardly changed (Table 1), which

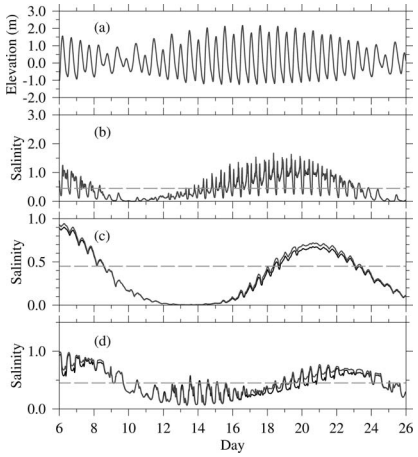

Figure 7. Modeled temporal variation of the elevation at the water intake of the Qingcaosha Reservoir (a) and the surface salinity at the water intakes of the Dongfengxisha Reservoir (b), Chenhang Reservoir (c), and Qingcaosha Reservoir (d) before and after the project from 6 February to 26 February in 2014. The dashed line is 0.45, which is the standard salinity of drinking water.

means that the influence of the project on the saltwater intrusion in the North Branch is very small during neap tide.

DISCUSSION

The water resources in the Changjiang Estuary are closely related with the saltwater intrusion. The saltwater intrusion at the water intakes of three reservoirs disappears in summer because of large river discharge, but it frequently occurs in winter because of low river discharge. Previous studies showed that the salinities at the Dongfengxisha Reservoir and Chenhang Reservoir were totally influenced by the saltwater spillover but that the Qingcaosha Reservoir is mainly threatened by the saltwater spillover and impacted by the saltwater intrusion from the North Channel (Chen and Zhu, 2014; Lyu and Zhu, 2018).

The temporal variations in the surface salinity and tidally averaged salinity of four tidal patterns at the water intakes of the Dongfengxisha Reservoir, Chenhang Reservoir, and Qingcaosha Reservoir before and after the project are shown in Figure 7 and Table 4. The temporal variations in the salinity show that semidiurnal flood and ebb periods occur and that semimonthly spring and neap period variations are induced by the tides. At the water intake of the Dongfengxisha Reservoir, the salinity is higher during the spring and middle tides after the spring tide, and the salinity is lower during the neap and middle tides after the neap tide. The duration that the salinity is lower than 0.45 psu is about half of the time, which is the salinity standard for drinking water, and the reservoir has enough time to receive water from the Changjiang Estuary. Before the RP-EHS, the tidally averaged surface salinity at the water intakes of the Dongfengxisha Reservoir during spring tide, middle tides after the spring tide, neap tide, and middle tides after the neap tide are 0.69, 0.77, 0.10, and 0.31 psu, respectively. At the water intake of the Chenhang Reservoir,

Table 4. *Tidally averaged salinity during four tidal patterns at the water intakes of the Dongfengxisha Reservoir, Chenhang Reservoir, and Qingcaosha Reservoir before and after the RP-EHS.*

	Spring	MTST	Neap	MTNT
DFXSR				
Before	0.69	0.77	0.1	0.31
After	0.72	0.79	0.1	0.32
$\triangle_{\text{After-Before}}$	0.03	0.02	0	0.01
CHR				
Before	0.19	0.63	0.25	0.01
After	0.22	0.67	0.25	0.01
$\triangle_{\text{After-Before}}$	0.03	0.04	0	0
QCSR				
Before	0.26	0.56	0.48	0.25
After	0.3	0.63	0.48	0.25
$\triangle_{\text{After-Before}}$	0.04	0.07	0	0

the duration that the salinity is lower than 0.45 psu is longer than two-thirds of the time. Comparing the salinity peak phase with that of the Dongfengxisha Reservoir, you can see that it takes approximately 2 days for the saltwater to move from the water intake of the Dongfengxisha Reservoir to the water intake of the Chenhang Reservoir. Before the RP-EHS, the tidally averaged surface salinities at the water intake during spring tide, middle tides after the spring tide, neap tide, and middle tides after the neap tide are 0.19, 0.63, 0.25, and 0.01 psu, respectively, meaning that water resources are optimistic in the Chenhang Reservoir except during MTSP. At the water intake of the Qingcaosha Reservoir, salinity is lower than 0.45 psu about half of the time. Before the RP-EHS, the tidally averaged surface salinities at the water intake during spring tide, middle tides after the spring tide, neap tide, and middle tides after the neap tide are 0.26, 0.56, 0.48, and 0.25 psu, respectively, meaning that water resources are optimistic in the Qingcaosha Reservoir except during MTSP and neap tide.

As mentioned previously, the saltwater intrusion in the North Branch and the saltwater spillover are somewhat enhanced by the RP-EHS, which results in the salinity at the water intakes of the Dongfengxisha Reservoir, Chenhang Reservoir, and Qingcaosha Reservoir being increased slightly (Figure 7b–d). Because the saltwater sources are mainly from the saltwater spillover, the salinity is increased by 0.03, 0.02, 0.01, and 0.01 psu at the water intake of the Dongfengxisha Reservoir by 0.03, 0.04, 0.00, and 0.00 psu at the water intake of the Chenhang Reservoir and by 0.04, 0.07, 0.00, and 0.00 psu at the water intake of the Qingcaosha Reservoir during spring tide, middle tides after the spring tide, neap tide, and middle tides after the neap tide, respectively. This means that the project is unfavorable for the water intake of the three reservoirs in the Changjiang Estuary.

Although the RP-EHS impacts on the freshwater at the reservoir water intakes are somewhat small, the conclusion is obtained from the simulation with climatological states of river discharge and wind. Low river discharge and strong northerly winds occur occasionally during winter, which can enhance the saltwater intrusion and severely threaten water resources (Li, Zhu, and Wu, 2012). The combined effects of tidal flat reclamation, low river discharge, and strong northerly winds should be considered to ensure water safety for Shanghai in the future.

CONCLUSIONS

A well-validated numerical model was used to simulate the influences of the RP-EHS on saltwater intrusion and freshwater in the Changjiang Estuary. The residual water transport, salt transport, and WDR were used to analyze the effects of the project. Before the RP-EHS, the surface RUWF flows were seaward in the South Branch, North Channel, North Passage, and South Passage, landward in the North Branch, and northward east of Chongming Island because of tidal Stokes transport and pumping transport during spring tide. The bottom RUWF at the river mouth is landward induced because of a strong salinity front. The RUSF pattern is similar to that of the RUWF, while its magnitude out of the river mouth is much larger because of high salinity. During neap tide, the RUWF and RUSF flow southward out of the river mouth in the surface layer and even in the bottom layer because the tide becomes weaker and the effect of the north wind is dominant. The tidally averaged surface salinity at the water intakes during spring tide, middle tides after the spring tide, neap tide, and middle tides after the neap tide are 0.69, 0.77, 0.10, and 0.31 psu at the Dongfengxisha Reservoir; 0.19, 0.63, 0.25, and 0.01 psu at the Chenhang Reservoir; and 0.26, 0.56, 0.48, and 0.25 psu at the Qingcaosha Reservoir, respectively. There is enough time for the freshwater from the Changjiang Estuary to flow into the reservoirs.

Since the establishment of RP-EHS, the model-simulated NTWF and WDR in the North Channel have increased by 888 m^3/s and 7.9% during spring tide, which means more river water is bifurcated into the North Channel. Consequently, the salinity is decreased. Another reason is that the RP-EHS lengthens the North Channel, which leads the lower salinity water to flow further east. Salinity is increased to a maximum value of more than 1.0 psu in the Eastern Chongming Shoal because the RUWF and RUSF are enhanced, which can bring high salinity to that area. In the South Channel, North Passage and South Passage, NTWF is decreased by 869, 626, and 241 m^3/s, which results in a salinity increment of approximately 1.0 psu. At the upper reaches of the North Branch, the NTWF, which spills over from the North Branch into the South Branch, is increased by 15 m^3/s, and the WDR rises by 0.2%, indicating that the RP-EHS somewhat enhances the saltwater intrusion in the North Branch and the saltwater spillover. During neap tide, the changes in NTWF, WDR, and salinity in each channel are smaller than the changes that occur during spring tide. The saltwater intrusion in the North Branch and the saltwater spillover are somewhat enhanced by the RP-EHS. The salinity at the water intakes of the Dongfengxisha Reservoir, the Chenhang Reservoir, and Qingcaosha Reservoir is increased slightly because the saltwater in the water intakes is mainly from the saltwater spillover. The salinities at water intakes during spring tide, middle tides after the spring tide, neap tide, and middle tides after the neap tide are increased by 0.03, 0.02, 0.01, and 0.01 psu at the Dongfengxisha Reservoir; 0.03, 0.04, 0.00, and 0.00 psu at the Chenhang Reservoir; and 0.04, 0.07, 0.00, and 0.00 psu at the Qingcaosha Reservoir, respectively. This means that the project is unfavorable for the water intake of the three Changjiang Estuary reservoirs. The reservoirs are important for Shanghai's water supply, and the effects of the

tidal flat reclamation on water resources should receive more attention to ensure water safety.

ACKNOWLEDGMENTS

This work was supported by the National Natural Science Foundation of China (41676083), Major Program of Shanghai Science and Technology Committee (17DZ1201902), and Shanghai Institute of Eco-Chongming. We thank the anonymous reviewers for their constructive suggestions.

LITERATURE CITED

Andrews, S.W.; Gross, E.S., and Hutton, P.H., 2017. Modeling salt intrusion in the San Francisco Estuary prior to anthropogenic influence. *Continental Shelf Research*, 146, 58–81.

Blumberg, A.F., 1994. A primer for ECOM-si. Technical Report of HydroQual, 66p.

Blumberg, A.F. and Mellor, G.L., 1987. A description of a three-dimensional coastal ocean circulation model. *Coastal and Estuarine Science*, 4, 1–16.

Chen, J. and Zhu, J.R., 2014. Sources for saltwater intrusion at the water intake of Qingcaosha Reservoir in the Changjiang Estuary. *Acta Oceanologica Sinica*, 36(11), 131–141.

Chen, C.; Zhu, J.; Zheng, L.; Ralph, E., and Budd, J.W., 2004. A non-orthogonal primitive equation coastal ocean circulation model: Application to Lake Superior. *Journal of Great Lakes Research*, 30(1), 41–54.

Editorial Board for Marine Atlas, 1992. *Ocean Atlas in Huanghai Sea and East China Sea (Hydrology)*. Beijing: China Ocean, pp. 19–45.

Galperin, B.; Kantha, L.H.; Hassid, S., and Rosati, A., 1988. A quasi-equilibrium turbulent energy model for geophysical flows. *Journal of the Atmospheric Sciences*, 45(1), 55–62.

Geyer, W.R. 1993. The importance of suppression of turbulence by stratification on the estuarine turbidity maximum. *Estuaries*, 16, 113–125.

Li, L.; Zhu, J.R., and Wu, H., 2012. Impacts of wind stress on saltwater intrusion in the Yangtze Estuary. *Science China Earth Sciences*, 55(7), 1178–1192.

Li, L.; Zhu, J.R.; Wu, H., and Guo, Z.G., 2014. Lateral saltwater intrusion in the North Channel of the Changjiang Estuary. *Estuaries and Coasts*, 37(1), 36–55.

Li, L.; Zhu, J.R.; Wu, H., and Wang, B., 2010. A numerical study on water diversion ratio of the Changjiang (Yangtze) estuary in dry season. *Chinese Journal of Oceanology and Limnology*, 28(3), 700–712.

Lyu, H.H. and Zhu, J.R., 2018. Impact of the bottom drag coefficient on saltwater intrusion in the extremely shallow estuary. *Journal of Hydrology*, 557, 838–850.

Manda, A. and Matsuoka, K., 2006. Changes in tidal currents in the Ariake Sound due to reclamation. *Estuaries and Coasts*, 29(4), 645–652.

Mellor, G.L. and Yamada, T., 1982. Development of a turbulence closure model for geophysical fluid problems. *Reviews of Geophysics*, 20(4), 851–875.

Okada, T.; Nakayama, K.; Takao, T., and Furukawa, K., 2011. Influence of freshwater input and bay reclamation on long-term changes in seawater residence times in Tokyo bay, Japan. *Hydrological Processes*, 25(17), 2694–2702.

Pritchard, D.W., 1956. The dynamic structure of a coastal plain estuary. *Journal of Marine Research*, 33–42.

Qiu, C. and Zhu, J.-R., 2013. Influence of seasonal runoff regulation by the Three Gorges Reservoir on saltwater intrusion in the Changjiang River Estuary. *Continental Shelf Research*, 71, 16–26.

Qiu, C. and Zhu, J.R., 2015. Assessing the influence of sea level rise on salt transport processes and estuarine circulation in the Changjiang River estuary. *Journal of Coastal Research*, 31(3), 661–670.

Qiu, C.; Zhu, J.R., and Gu, Y.L., 2012. Impact of seasonal tide variation on saltwater intrusion in the Changjiang River estuary. *Chinese Journal of Oceanology and Limnology*, 30(2), 342–351.

Shen, H.T.; Mao, Z.C., and Zhu, J.R., 2003. *Saltwater Intrusion in the Changjiang Estuary*. Beijing: China Ocean, 175p.

Saha, S.; Moorthi, S.; Pan, H.L.; Wu, X.; Wang, J.; Nadiga, S.; Tripp, P.; Kistler, R.; Woollen, J.; Behringer, D.; Liu, H.; Stokes, D.; Grumbine, R. Gayno, G.; Wang, J.; Hou, Y.-T.; Chuang, H.-Y.; Juang, H.-M.; Sela, J.; Iredell, M.; Treadon, R.; Kleist, D.; van Delst, P.; Keyser, D.; Derber, J.; Ek, M.; Meng, J.; Wei, H.; Yang, R.; Lord, S.; van den Dool, H.; Kumar, A.; Wang, W.; Long, C.; Chelliah, M.; Xue, Y.; Huang, B.; Schemm, J.-K.; Ebisuzaki, W.; Lin, R.; Xie, P.; Chen, M.; Zhou, S.; Higgins, W.; Zou, C.-Z.; Liu, Q.; Chen, Y.; Han, Y.; Cucurull, L.; Reynolds, R.W.; Rutledge, G., and Goldberg, M., 2010. The NCEP climate forecast system reanalysis. *Bulletin of the American Meteorological Society*, 91(8), 1015–1058.

Simpson, J.H.; Brown, J.; Matthews, J., and Allen, G., 1990. Tidal straining, density currents, and stirring in the control of estuarine stratification. *Estuaries and Coasts*, 13(2), 125–132.

Song, D.; Wang, X.H.; Zhu, X., and Bao, X., 2013. Modeling studies of the far-field effects of tidal flat reclamation on tidal dynamics in the East China Seas. *Estuarine Coastal & Shelf Science*, 133(4), 147–160.

van Maren, D.S.; Oost, A.P.; Wang, Z.B., and Vos, P.C., 2016. The effect of land reclamations and sediment extraction on the suspended sediment concentration in the Ems Estuary. *Marine Geology*, 376, 147–157.

Wu, H.; Shen, J.; Zhu, J.R.; Zhang, J., and Li, L., 2014. Characteristics of the Changjiang plume and its extension along the Jiangsu Coast. *Continental Shelf Research*, 76(2), 108–123.

Wu, H. and Zhu, J.R., 2007. Analysis of the transport mechanism of the saltwater spilling over from the North Branch in the Changjiang Estuary in China. *Acta Oceanologica Sinica*, 1, 17–25.

Wu, H. and Zhu, J., 2010. Advection scheme with 3rd high-order spatial interpolation at the middle temporal level and its application to saltwater intrusion in the Changjiang Estuary. *Ocean Modelling*, 33(1–2), 33–51.

Wu, H.; Zhu, J.R.; Chen, B.R., and Chen, Y.Z., 2006. Quantitative relationship of runoff and tide to saltwater spilling over from the North Branch in the Changjiang Estuary: A numerical study. *Estuarine, Coastal & Shelf Science*, 69(1–2), 125–132.

Wu, H.; Zhu, J.R., and Choi, B.H., 2010. Links between saltwater intrusion and subtidal circulation in the Changjiang Estuary: A model-guided study. *Continental Shelf Research*, 30(17), 1891–1905.

Zainal, K.; Al-Madany, I.; Al-Sayed, H.; Khamis, A.; Al Shuhaby, S.; Al Hisaby, A.; Elhoussiny, W., and Khalaf, E., 2012. The cumulative impacts of reclamation and dredging on the marine ecology and land-use in the Kingdom of Bahrain. *Marine Pollution Bulletin*, 64(7), 1452–1458.

Zhang, H.; Zhu, J.-R., and Wu, H., 2005. Numerical simulation of eight main tidal constituents in the East China Sea, Yellow Sea and Bohai Sea. *Journal of East China Normal University*, 3, 71–77.

Zheng, L.Y.; Chen, C.S., and Liu, H.D., 2003. A modeling study of the Satilla River Estuary, Georgia. I: Flooding-drying process and water exchange over the salt marsh-estuary-shelf complex. *Estuaries*, 26(3), 651–669.

Zheng, L.Y.; Chen, C.S., and Zhang, F.Y., 2004. Development of water quality model in the Satilla River Estuary, Georgia. *Ecological Modelling*, 178(3–4), 457–482.

Zhu, J.R.; Ding, P.X.; Zhang, L.Q.; Wu, H., and Cao, H.J., 2006. Influence of the deep waterway project on the Changjiang Estuary. *In:* Wolanski, E. (ed.), *The environment in Asia Pacific Harbours*. Netherlands: Springer, pp. 79–92.

Zhu, J.-R.; Wu, H.; Li, L., and Wang, B., 2010. Saltwater intrusion in the Changjiang Estuary in the extremely drought hydrological year 2006. *Journal of East China Normal University (Natural Science)*, 4(1), 1–6.